Responses to the Reviewer's Comment

We thank the reviewer for the constructive and insightful comment. Our point-by-point responses can be found below, with reviewer comments in **black**, our responses in **blue**, alongside the relevant revisions to the manuscript in **red**.

RC#2

The manuscript by Gao et al. reported the near-complete speciation of reactive organic gases (ROGs) with 125 species identified to evaluate their emission characteristics from residential combustion. The authors used a Gas Chromatography equipped with a Mass Spectrometer and a Flame Ionization Detector (GC-MS/FID) and H_3O^+/NO^+ Proton Transfer Reaction Time-of- Flight Mass Spectrometer (Vocus PTR-ToF-MS) to identify 55 previously un- and under-characterized species. Without considering these "newly identified species", the ROG emissions from residential coal and biomass combustion would be underestimated by 44.3% ± 11.8% and 22.7% ± 3.9%, respectively, which further highlighted the potential underestimation of secondary organic aerosols formation potential (SOAP) and OH reactivity (OHR) of ROG emissions. Overall, this study would be a useful addition to better understanding the detailed speciation of ROGs from residential combustion. However, the novelty of this study should be clearly addressed, especially given that some previous studies also applied these advanced instruments and have identified these "newly identified species" (Figure 2).

R:

ROG emissions from residential combustion especially biomass combustion have been widely studied due to their great contribution to global ROGs and the complexity of compositions. Among them, studies focusing on the ROG speciation for residential combustion could generally be divided into three categories according to the measurement methods, as listed in Table R1. The first one was the whole-air sampling with offline analysis by one-dimensional gas chromatography system equipped with a mass spectrometer and/or a flame ionization detector (GC-MS/FID), which mainly focused on the hydrocarbons (<C12) (Mo et al., 2016; Wang et al., 2013; Liu et al., 2008). With the development of the advanced instruments, the second category of studies on ROG emissions gave more attention to the polar species like oxygenated ROGs, which could be online detected through the whole combustion process mainly by proton transfer reaction time-of-flight mass spectrometry (H_3O^+ PTR-ToF-MS) due to the high mass resolution and sensitivity (Cai et al., 2019; Bruns et al., 2017; Stockwell et al., 2015; Koss et al., 2018; Akherati et al., 2020; Wu et al., 2022). Considerable (approximately 6%-24%) species with intermediate volatility in residential ROG emissions were identified as the large contributors of secondary organic aerosols (SOA) (Cai et al., 2019; Koss et al., 2018).

Thirdly, due to the inability to isolate isomers by H_3O^+ PTR-ToF-MS and considerable amount of oxygenated ROGs with intermediate volatility in residential ROG emissions, the increasing interest has been put on the application and comparisons of multiple instruments for the detailed identification of ROG species (Koss et al., 2018; Hatch et al., 2017). More than 150 PTR ion masses

were identified using the combination of techniques including GC pre-separation, two-dimensional GC system (GC×GC), fourier transform infrared spectroscopy (FTIR), and NO^+ chemical ionization mass spectrometer (NO^+ CIMS), which contributed ~90% of the ROG masses detected by H_3O^+ PTR-ToF-MS in biomass combustion emissions (Koss et al., 2018). The comparisons demonstrated that H_3O^+ PTR-ToF-MS might be the most suitable for the detection of the lowest-volatility and most polar species, which covered the most (50%-79%) species, comparing with the other instruments, in the combined ROG measurement covering more than 500 species from different instruments (Koss et al., 2018; Hatch et al., 2017).

Recently, the higher alkanes (≥C8), one kind of considerable species in residential combustion emissions (Jathar et al., 2014; Huo et al., 2021; Li et al., 2023), which were not included in the comprehensive measurements of previous studies (Hatch et al., 2017), could be well measured by PTR-ToF-MS with NO^+ ion chemistry (Wang et al., 2020; Koss et al., 2016). Thus, PTR-ToF-MS might be a preferent and promising method for the development of near-complete ROG speciation relevant for residential combustion, but need to combine with GC-MS/FID for the complement measurement of aliphatic hydrocarbons. Compared to the comprehensive measurements by more instruments previously, the combination of PTR-ToF-MS and the GC-MS/FID method was labor-saving and further could minimize the measurement uncertainties from the synthesis of measurement data due to fewer kinds of instruments. Therefore, the present study focused on (1) developing the near-complete ROG speciation through quantifying all signals by H_3O^+ PTR-ToF-MS and supplementing C2-C22 aliphatic hydrocarbons by GC-MS/FID and NO^+ PTR-ToF-MS, and (2) the composition of ROG emissions through the real combustion sampling in rural household of China. Finally, the near-complete ROG speciation further supported the estimation of the ROG emissions from residential combustion in China as well as their hydroxy radical reactivity and formation potential of SOA. The present study took the residential combustion as an example for developing the near-complete ROG speciation mainly considering the large complexity of combustion-relevant ROG speciation and the comprehensive measurement of residential combustion previously, which could be used to further confirm the present result by overlapping species.

We have revised it in the sections of Abstract and Introduction in the revised manuscript.

Table R1 Review on the measurements of ROG emissions from residential combustion.

Method	Fuel types	Reference	Numbers of species		
			GC-MS/ FID	PTR-ToF-MS	Other instruments
Combustion in stove	Residential coals, biomass (straw and wood) from China	This study	71	84 (84-92% of the overall peak mass)	—
	Corncob from China	(Wu et al., 2022)	—	13	—
	Anthracite, bituminous coal from China	(Cai et al., 2019)	—	79-89 (90-96% of the overall peak intensities)	—
	Beech (Fagus sylvatica) logs	(Bruns et al., 2017)	—	64 (94-97% of the total mass)	—
	Biomass (peanut shell, maize straw), raw	(Wang et al., 2013)	60	—	24 (DNPH-HPLC [a])

Method	Fuel types	Reference	Numbers of species		
			GC-MS/ FID	PTR-ToF-MS	Other instruments
	coals from China				
Combustion simulation in Lab	Biomass fuels from the western US	(Akherati et al., 2020)	—	150	—
	Burned fuels from the western US	(Koss et al., 2018)	—	172 (~95% of the overall peak intensities)	15 (FTIR [b]), 261(GC-CIMS [c])
	Four burns: ponderosa pine boughs, Chinese rice straw, Indonesian peat, and black spruce boughs	(Hatch et al., 2017)	~27	~71	~13 (FTIR) ~418 (GC×GC)
	Authentic globally significant fuels	(Stockwell et al., 2015)	—	46-92	—
	Biomass burns of 18 fuel types from 3 geographic regions in the US	(Gilman et al., 2015)	187	Unpublished	Unpublished (FTIR)
	Residential coal, rice, maize, and wheat straw from China	(Mo et al., 2016)	62	—	13 (DNPH-HPLC)
	biomass, residential coal from China	(Liu et al., 2008)	92	—	—

Note:

[a], DNPH-HPLC: 2, 4-Dinitrophenyl hydrazine followed by high performance liquid chromatography (HPLC).

[b], FTIR: Fourier transform infrared spectroscopy.

[c], GC-CIMS: Gas chromatography chemical ionization mass spectrometry.

Specific issues:

Q1: Line 115-116: why only selected peaks (mainly higher alkanes) under NO^+ mode PTR measurements were studied?

R:

Multi-instruments were deployed to measure ROGs in the emissions of residential combustion, aiming to develop a near-complete speciation of ROGs in this study, which included H_3O^+ PTR-ToF-MS, NO^+ PTR-ToF-MS, and GC-MS/FID. H_3O^+ PTR-ToF-MS could identify the ROGs as long as the proton affinity of ROGs greater than that of water (691 kJ mol^{-1}) (Yuan et al., 2017), with relatively complete species coverage. It may be the preferred method toward ROG complete measurement, because most ROGs can be detected (Li et al., 2020; Krechmer et al., 2018) and the sensitivity for a given ROG can be calculated theoretically by H_3O^+ PTR-ToF-MS (Sekimoto et al., 2017).

Despite these advantages, H_3O^+ PTR-ToF-MS has two limitations related to the reagent ion chemistry. Firstly, the technique is insensitive to C2-C7 alkanes, ethene and acetylene with lower

proton affinity than water (Jobson et al., 2009). Here, these common constituents of urban atmospheres were well-measured by traditional technology such as GC/MS-FID. Secondly, higher alkanes (≥C8), one kinds of important contents of the fuel combustion (Huo et al., 2021; Jathar et al., 2014), were difficult to quantify by H_3O^+ PTR-ToF-MS due to fragments produced during the ionization process. NO^+ PTR-ToF-MS has been demonstrated to provide a supplementary measurement of higher alkanes (Wang et al., 2020; Koss et al., 2016).

Different from H_3O^+ PTR-ToF-MS by which the sensitivity for a given ROG can be calculated theoretically even without the standard for calibration, authentic standards are necessary for quantification by NO^+ PTR-ToF-MS, which limited the characterization of mass spectrum ionized by NO^+. The difficulty to predict the ionized ROG products and to interpret the mass spectrum further limited its application in ROG speciation, because NO^+ has three common reaction mechanisms with ROGs: charge transfer, hydride abstraction, and cluster formation. Therefore, NO^+ PTR-ToF-MS in this study was only used for a supplementary measurement of higher alkanes (≥C8) with a reported well-established quantitative method (Wang et al., 2020).

Q2: Line 151: the loss of acids and alcohols in the canister is larger, and the author attributed this to their functional groups of -COOH and -OH. Would it be more direct to relate this to the volatility of compounds? Are there any criteria to exclude these compounds from the analysis?

R:

The loss of ROGs in the canisters during storage mainly relate to their volatility and polarity. As shown in Fig. R1(a), there was no significant dependence of the loss proportion on the volatility (the effective saturation vapor concentration, C^*) of ROGs in current experimental results for 10 days. The species with similar $\log_{10}C^*$ had largely different loss fractions and the loss fraction of the species with increased $\log_{10}C^*$ didn't reduced regularly as expected. The higher polarity of alcohols is a possible reason for their larger loss proportion in Fig. R1(b), as polar species preferentially adsorbed on surface sorption sites of SUMMA canister inner walls (Batterman et al., 1998). Considering the rough rank of functional groups involved in this study from high polarity to low polarity (-COOH, -OH, -CN, -NO_n, -CHO, RCO- and single/double/triple bond), species with higher polarity like acids and alcohols might have larger loss proportion, which were excluded from the analysis.

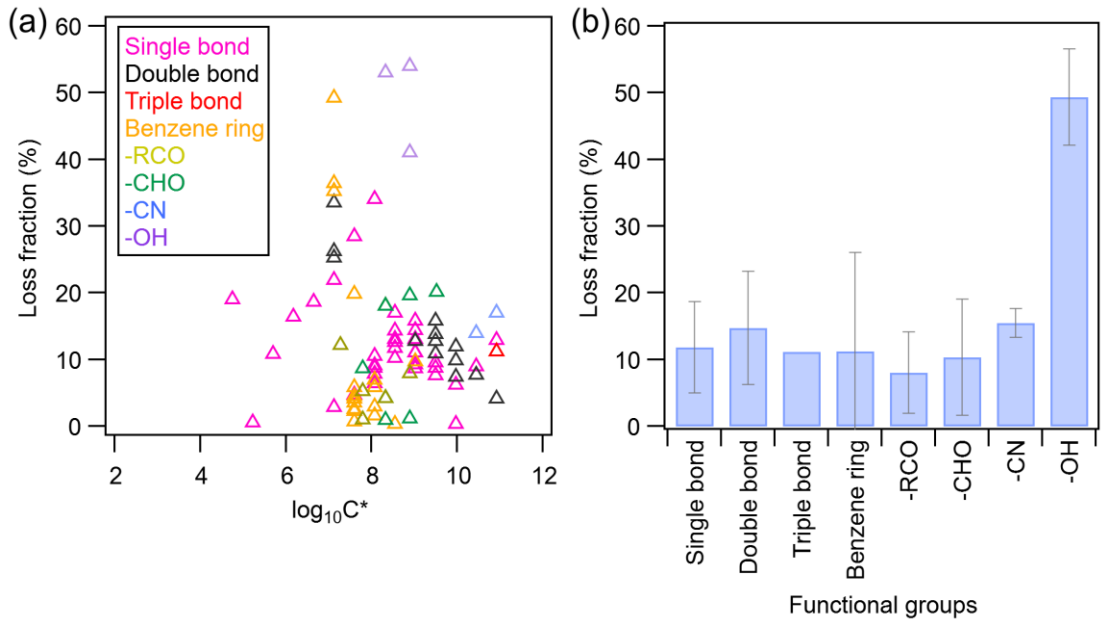

Figure R1. Plots of the loss fraction versus volatility (the logarithmic effective saturation vapor concentration, $\log_{10}C^*$) and polarity (functional groups) of species respectively. (a) The scatter plot of the loss fractions of individual species and $\log_{10}C^*$, colored by functional groups (see legend). (b) The average and standard deviation of loss fraction for species with the same functional groups.

To clarify, the critera to exclude these compounds from the analysis were added in Section 2.2.3 of the main text as following. Briefly, loss in storage were estimated, and the species with unknown loss proportion or large loss proportion higher than 50% were just used to quantify the total ROGs and were excluded in the detail speciation of ROGs.

"According to experimental results, … the loss of several alcohols (-OH) exceeded 50%. The higher polarity of alcohols is a possible reason for their larger loss proportion, as the polar species preferentially adsorbed on surface sorption sites of SUMMA canister inner walls (Batterman et al., 1998). Although volatility is another potential factor, in current experimental results for 10 days, the loss proportion has no significant dependence on volatility (Fig. S4).

For the other species such as acids (-COOH), … there were no standards used to evaluate the loss during storage. Overall, 63 specific ROGs with large uncertainty potentially (>50%) and 861 unknown masses with uncertain loss fraction were only used to quantify the total ROGs and were excluded from the further discussion of ROG composition."

Q3: Line 174 and 324: why is benzene chosen for normalization purposes?

R:

The detailed speciation of ROG emissions from residential combustion was studied comprehensively by PTR-ToF-MS combining with GC-MS/FID, while the measurement of formaldehyde and the emission factors (EFs) of ROGs were not included in our experiments. Thus, the normalization of the ROG speciation in this study was for two purposes. One was to include the

contribution of formaldehyde in the near-complete speciation of ROGs, which has been reported as one important species with considerable contribution in ROGs from residential combustion emissions (Cheng et al., 2022; Gilman et al., 2015). The other was to estimate the EFs of the newly identified species, which were rarely reported in previous studies. Both the above two purposes could be achieved by the normalization of the emission ratios of the target species (i.e. formaldehyde for the first purpose, and the newly identified species for the second purpose) with the reference species in emissions, which derived from the measurements in the present study.

Generally, all the overlapping species measured in this and the previous studies could be used for the above purpose, because the relative contribution of all the overlapping species agreed well between the current study and the previous studies as presented in Fig. S6 in the Supplementary Information. As shown in Fig. S6, the ROG species reported in different studies were various, among which aromatics were the major overlapping species in all the studies. Hence, aromatics including benzene were firstly selected as the potential reference species. Secondly, benzene was the most abundant aromatic species in the emissions of all types of fuel combustion as listed in Table S5 in the Supplementary Information, suggesting a relative lower uncertainty of the EF compared to other aromatics in previous studies. Meanwhile, the measurement of benzene in our study was also with a relative low uncertainty of 11%. Given the abovementioned, benzene was used as the reference species for the normalization.

Still, we tested other species with reported EFs and the derived EFs of ROGs with different reference species were presented in Fig. S12 in the Supplementary Information. As shown, the uncertainty of the estimated EFs of newly identified ROGs among different tests ranged from 4% (6%) to 39% (26%) for straws (coals) combustion.

We have clarified it more clearly in Section 2.3 and 3.2 in the revised manuscript, as following:

Section 2.3.4, line 235-241:

"To include the contribution of formaldehyde in the near-complete speciation of ROGs, the emission ratio of formaldehyde with the reference species in emissions was effective for this purpose. Generally, all the overlapping species measured in this and the previous studies could be used as the reference species, because the relative contribution of all the overlapping species agreed well between the current study and the previous studies as presented in Fig. S6 in the Supplementary Information. Benzene was chosen for normalization because in the emissions of all types of fuel combustion, benzene was the most abundant aromatics that were the major overlapping species between the current and previous studies."

Section 3.3, line 395-408:

"Here, benzene as well as its reported EF was used for the purpose above, as benzene was the major overlapping species in all the studies with the high abundance and a relative low uncertainty in combustion emission. We also tested other major species with reported EFs (Fig. S12). …There were no significant differences (-39%-4% for straws and 6%-26% for coals) of the estimated EFs of newly identified ROGs among different tests, which further confirmed our results were comparable with the previous studies but with more ROG species measured, as shown in Fig. S12."

Q4: Figure S2 (b): how many compounds were used here, and why were they chosen for comparison but not all the compounds?

R:

A total of 18 standard gases were used to calibrate the H_3O^+ PTR-ToF-MS in this study, which were all used for the comparison of calculated and measured sensitivities by H_3O^+ PTR-ToF-MS, as presented in Fig. S2 in the Supplementary Information.

We have clarified it more clearly in the revised Supplementary Information.

Q5: Given this study is based on offline analysis that some dynamic changes in emissions from residential combustion may not be reflected. Could this cause a potential bias?

R:

Generally, a combustion cycle mainly comprised four stages: ignition, flaming, smoldering and ember. The emissions as well as the speciation might have some dynamic changes through the process with the change of combustion conditions. The ROG composition and individual species proportion in source profiles obtained in the present study were mainly from the measurements during the flaming stage. Thus, for the present ROG composition and individual species proportion, the potential bias was related to their difference between flaming stage and the whole combustion cycle.

(1) Coal combustion

As reported in Cai et al. (2019), the emitted ROGs in the four stages accounted for 20%, 46%, 30%, and 4% of the total emissions throughout the whole cycle, respectively. The hydrocarbons which were primarily generated by pyrolysis of the volatile matter in coal, dominated the first two phases. With the increasing combustion efficiency in both the flaming and smoldering phases, the number of oxidized forms of hydrocarbons increased. The percentages of oxygenated ROGs like carbonyls and acids increased throughout the combustion cycle, while the fraction of oxygenated aromatics decreased when approaching the last stage of combustion. The fraction of N-containing ROGs increased throughout the combustion process. In summary, the composition of ROGs in each stage was shown in Fig. R2, as well as the weighted average composition during the whole cycle. The ROG composition in flaming stage and the whole cycle agreed well (Table R2), which was expected due to the small changes of ROG composition throughout the first three stages which emitted 96% of ROGs. Furthermore, by re-analyzing the data obtained from the authors, the proportion of individual species between the flaming stage and the whole cycle has a deviation varying from -50% (formic acid, CH_2O_2) to 22% (nitromethane, CH_3NO_2) for coal combustion (Fig. R4). From this point of view, for residential coal combustion, the bias of the ROG composition obtained in our study was negligible and the bias of the individual species proportion was within 50% generally.

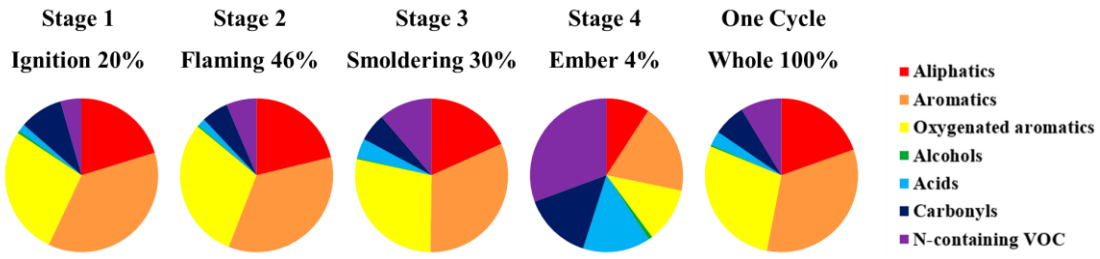

Figure R2. Average ROG compositions for residential coal combustion at each stage and the whole cycle adapted from Cai et al. (2019) (The figure was redrawn using the data from the authors).

(2) Biomass combustion

Using the available time-resolved data of ROGs emitted from straw combustion reported by Koss et al. (2018), a re-analysis similar to coals above was conducted. The emitted ROGs in the four stages accounted for 30%, 43%, 21%, and 6% of the total emissions throughout the whole cycle, respectively. Carbonyls dominated the first three phases (41%~45%) with a decrease by ~7% during the last stage. The percentages of other oxygenated ROGs like oxygenated aromatics increased from 3% to 7% throughout the combustion cycle, while the fraction of furans (11%~14%) and esters (~1%) remained relatively stable throughout the combustion cycle. Hydrocarbons showed a similar stable contribution (8%~12%). The fraction of N-containing ROGs increased from 1% to 4% throughout the combustion process. In summary, the composition of ROGs in each stage was shown in Fig. R3, as well as the weighted average composition during the whole cycle. As presented, the ROG composition in flaming stage and the whole cycle agreed well (Table R2), which was expected due to the small changes of ROG composition throughout stage 2 and stage 3 which emitted 64% of ROGs. Furthermore, the proportion of individual species between the flaming stage and the whole cycle has a deviation ranging from -47% (formic acid, CH_2O_2) to 22% (benzene, C_6H_6) except nitromethane (109%) for straw combustion (Fig. R4). The previous study of Gilman et al. (2015) have carefully compared discrete emission ratios (ERs) during flaming and smoldering combustion and fire-integrated ERs of the whole cycle and the average slope and standard deviation of discrete versus fire-integrated ERs for select ROGs from 56 biomass burns in the US was 1.2 ± 0.2 (Gilman et al., 2015). From this point of view, the bias of the ROG composition of biomass combustion obtained in our study was negligible and the bias was estimated to be within 50% generally in terms of individual species.

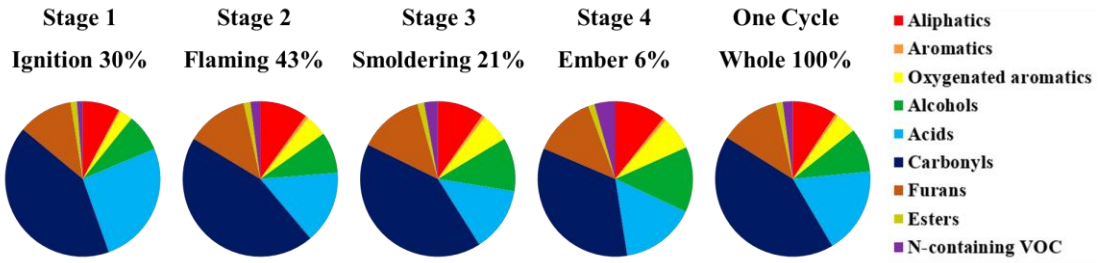

Figure R3. Average ROG compositions for straw combustion experiments at each stage and the whole cycle redrawn using data from Koss et al. (2018) (available data from the CSD NOAA archive at https://esrl.noaa.gov/csd/groups/csd7/measurements/2016firex/FireLab/DataDownload/ (NOAA, 2018)).

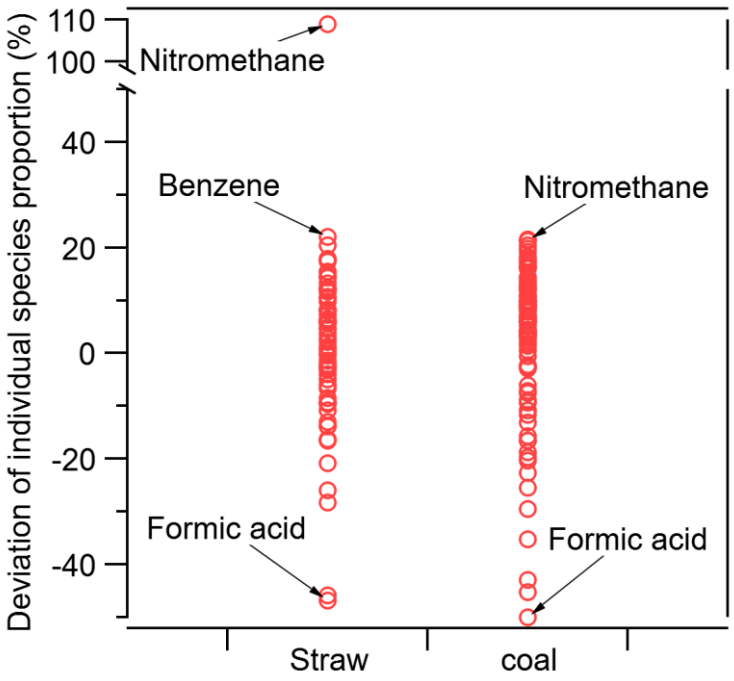

Figure R4. The deviation of the proportion of individual species between the flaming stage and the whole cycle. Only the points with the upper and lower limits of deviation and outlies are marked by the species name.

Table R2. Comparison of average ROG compositions and the relative deviation for residential coal and straw combustion between the flame stage and the whole cycle adapted from Cai et al. (2019) and Koss et al. (2018).

Fuel	**Coal**			**Straw**		
Stage	**Flaming**	**Cycle**	**Relative deviation**	**Flaming**	**Cycle**	**Relative deviation**
Aliphatics	21%	20%	5%	10%	9%	11%
Aromatics	35%	33%	6%	1%	1%	0%
Oxygenated aromatics	30%	28%	7%	4%	4%	0%
Alcohols	0%	0%	0%	9%	9%	0%
Acids	2%	3%	-33%	15%	18%	-17%
Carbonyls	6%	7%	-14%	45%	42%	5%
N-containing VOC	6%	9%	-33%	2%	2%	0%
Furans	/	/	/	13%	13%	0%
Esters	/	/	/	1%	1%	0%

Note: "/" means no reported data in the reference.

In summary, the bias of the fractions of species categorized by functional group from both coal and biomass combustion obtained in our study was negligible, and the bias of individual species proportion from both coal and biomass was estimated to be within 50% generally.

We have provided the discussions above in Section 3.1 in the revised manuscript as following.

Section 3.1, line 311-324:

"The ROG composition and individual species proportion in source profiles obtained in the present study were mainly from the measurements during the flaming stage. Considering the difference between flaming stage and the whole combustion cycle, the potential bias of the present results should be further discussed. By re-analyzing the data obtained from the authors (Cai et al., 2019) , the ROG composition from coal combustion in flaming stage and the whole cycle agreed well, which was expected due to the small changes of ROG composition throughout the first three stages which emitted 96% of ROGs (Fig. S9). Similar results (Fig. S10) could be concluded from the re-analysis of the reported emission data from biomass combustion by Koss et al. (2018) (Koss et al., 2018). Furthermore, the proportion of individual species between the flaming stage and the whole cycle has a deviation in the range of -50% to 22% for coal and straw combustion (Fig. S11). Actually, the previous study of Gilman et al. (2015) have carefully compared discrete emission ratios (ERs) during flaming and smoldering combustion and fire-integrated ERs of the whole cycle and the average slope and standard deviation of discrete versus fire-integrated ERs for select ROGs from 56 biomass burns in the US was 1.2 ± 0.2 (Gilman et al., 2015). In summary, the bias of the fractions of species categorized by functional group from both coal and biomass combustion obtained in our study was negligible, and the bias of individual species proportion from both coal and biomass was estimated to be within 50% generally."

Q6: Section 3.2: the SOA formation potential was estimated by using SOA yields from the literature. Are those values obtained at specific conditions? What would be the uncertainties for the estimation?

R:

(1) SOA yields

In order to estimate the SOA formation potential (SOAP) of ROGs from residential combustion, the SOA yield of observed species serving as a major parameter needs to be known. Among 80 SOA potential precursors in Table R3, the SOA yields of 44 species from previous chamber studies have been published, while SOA yields of nearly half potential precursors were still unknown.

The SOA yields in real atmosphere are dependent on nitrogen oxides (NO_x) level, total organic aerosol (OA) mass loading and temperature, etc., by modulating the chemical reaction pathway and phase partitioning. The SOA yields of 44 species mainly measured under high-NO_x conditions ($[NO_x] > 1$ ppb) except for benzenediols ($C_6H_6O_2$) and C2 phenols ($C_8H_{10}O$) from previous chamber studies were scaled to the ambient conditions ([OA] = 15.0 μg m^{-3}, T = 25 °C) (Gao et al., 2019) based on the two-product model (Ng et al., 2007; Li et al., 2016a) and further corrected for vapor wall losses (Zhang et al., 2014). Table R3 summarized the corrected SOA yields applied in this study and some details of chamber experiments (eg. the chamber yields and the numbers of experiments).

Potential precursors with unknown SOA yields include furans, phenols, 3-ring PAHs, terpenes except for α-pinene and alkanes with more than 6 carbon atoms especially branched alkanes. Alkanes containing 13, 14, 16 atoms were estimated using the reported two-product parameters (Presto et al., 2010) which derived from the experimental yields of C12 alkanes and C17 alkanes. SOA yields for other potential precursors were assumed as the corrected SOA yield of species with similar structure or the same number of carbon atoms applied in this study.

(2) The total uncertainty of SOAP

The overall uncertainty of estimated SOAP is related to the uncertainty of SOA yields and species proportions in source profiles. The yield uncertainty for corrected SOA yields from publications with at least 2 experiments was estimated to be within 11% according to the bias between two-product model fitting results and experimental yields. For other species with published SOA yield from only a single experiment or assumed SOA yields, the yield uncertainty has been estimated as ~50% (Bruns et al., 2016), which was cited in this study. The uncertainty of species proportion was 20% and 34% in coal and biomass combustion profiles, respectively, as mentioned in Section 2.3.4. Thus, the total uncertainty of SOAP could be calculated using error propagation function, being 32% and 41% for coal and biomass combustion, respectively.

We have added this discussion in Section 3.2 of the revised manuscript.

"Among 80 SOA potential precursors in Table S3, the SOA yields of 44 species from previous chamber studies have been published, while SOA yields of nearly half potential precursors were still unknown. The SOA yields in real atmosphere are dependent on nitrogen oxides (NO_x) level, total organic aerosol (OA) mass loading and temperature, etc., by modulating the chemical reaction pathway and phase partitioning. The SOA yields mainly measured under high-NO_x conditions ([NO_x] > 1 ppb) except for benzenediols ($C_6H_6O_2$) and C2 phenols ($C_8H_{10}O$) from previous chamber studies were scaled to the ambient conditions ([OA] = 15.0 μg m^{-3}, T = 25 °C) (Gao et al., 2019) based on the two-product model (Ng et al., 2007; Li et al., 2016a) and further corrected for vapor wall losses (Zhang et al., 2014). Table S3 summarized the corrected SOA yields applied in this study and some details of chamber experiments (eg. the chamber yields and the numbers of experiments). Potential precursors with unknown SOA yields include furans, phenols, 3-ring PAHs, terpenes except for α-pinene and alkanes with more than 6 carbon atoms especially branched alkanes. Alkanes containing 13, 14, 16 atoms were estimated using the reported two-product parameters (Presto et al., 2010) which derived from the experimental yields of C12 alkanes and C17 alkanes. SOA yields for other potential precursors were assumed as the corrected SOA yield of species with similar structure or the same number of carbon atoms applied in this study.

The overall uncertainty of estimated SOAP is related to the uncertainty of SOA yields and species proportions in source profiles. The yield uncertainty for corrected SOA yields from publications with at least 2 experiments was estimated to be within 11% according to the bias between two-product model fitting results and experimental yields. For other species with published SOA yield from only a single experiment or assumed SOA yields, the yield uncertainty has been estimated as ~50% (Bruns et al., 2016), which was cited in this study. The uncertainty of species proportion was 20% and 34% in coal and biomass combustion profiles, respectively, as mentioned in Section 2.3.4. Thus, the total uncertainty of SOAP could be calculated using error propagation function, being 32% and 41% for coal and biomass combustion, respectively."

Table R3. Applied SOA yields, chamber SOA yields, references and the numbers of experiments (N).

No.	Formula	Species	Applied Yield	Reference	Chamber Yield	N
1	C_2H_6	Ethane	/			
2	C_3H_8	Propane	/			
3	C_4H_{10}	Isobutane	/			
4	C_4H_{10}	n-Butane	/			

5	C_5H_{10}	Cyclopentane	/			
6	C_5H_{12}	Isopentane	/			
7	C_5H_{12}	n-Pentane	/			
8	C_6H_{12}	Methylcyclopentane	0.017	Assumed as Cyclohexane		
9	C_6H_{12}	Cyclohexane	0.017	(Lim and Ziemann, 2009)	0.040	1
10	C_6H_{14}	2,2-Dimethylbutane	/			
11	C_6H_{14}	2,3-Dimethylbutane	/			
12	C_6H_{14}	2-Methylpentane	/			
13	C_6H_{14}	3-Methylpentane	/			
14	C_6H_{14}	n-Hexane	0.000	(Lim and Ziemann, 2009)	0.000	1
15	C_7H_{14}	Methylcyclohexane	0.017	Assumed as Cyclohexane		
16	C_7H_{16}	2,4-Dimethylpentane	0.010	Assumed as n-Heptane		
17	C_7H_{16}	2-Methylhexane	0.010	Assumed as n-Heptane		
18	C_7H_{16}	2,3-Dimethylpentane	0.010	Assumed as n-Heptane		
19	C_7H_{16}	3-Methylhexane	0.010	Assumed as n-Heptane		
20	C_7H_{16}	n-Heptane	0.010	(Lim and Ziemann, 2009)	0.009	1
21	C_8H_{18}	2,2,4-Trimethylpentane	0.017	Assumed as n-Octane		
22	C_8H_{18}	2,3,4-Trimethylpentane	0.017	Assumed as n-Octane		
23	C_8H_{18}	2-Methylheptane	0.017	Assumed as n-Octane		
24	C_8H_{18}	3-Methylheptane	0.017	Assumed as n-Octane		
25	C_8H_{18}	n-Octane	0.017	(Lim and Ziemann, 2009; Presto et al., 2010)	0.041	1
26	C_9H_{20}	n-Nonane	0.021		0.070	1
27	$C_{10}H_{22}$	n-Decane	0.033		0.030-0.140	3
28	C_2H_4	Ethylene	/			
29	C_3H_6	Propylene	/			
30	C_4H_8	Trans-2-butene	/			
31	C_4H_8	1-Butene	/			
32	C_4H_8	Cis-2-butene	/			
33	C_5H_{10}	1-Pentene	/			
34	C_5H_{10}	Trans-2-pentene	/			
35	C_5H_{10}	Cis-2-pentene	/			
36	C_6H_{12}	1-Hexene	/			
37	C_2H_2	Acetylene	/			
38	C_6H_6	Benzene	0.096	(Li et al., 2016a; Ng et al., 2007)	0.078-0.349	8
39	C_7H_8	Toluene	0.200	(Li et al., 2016a; Ng et al., 2007)	0.078-0.196	12
40	C_8H_8	Styrene	0.016	(Tajuelo et al., 2019)	0.018-0.064	24
41	C_8H_{10}	Ethylbenzene	0.057	(Li et al., 2016a)	0.013-0.167	7
42	C_8H_{10}	m/p-Xylene	0.057	(Li et al., 2016a; Ng et al., 2007)	0.035-0.154	44
43	C_8H_{10}	o-Xylene	0.057	(Li et al., 2016a)	0.035-0.108	11
44	C_9H_{12}	iso-Propylbenzene	0.074	(Li et al., 2016a)	0.031-0.110	4
45	C_9H_{12}	n-Propylbenzene	0.074	(Li et al., 2016a)	0.051-0.054	2
46	C_9H_{12}	m-Ethyltoluene	0.074	(Li et al., 2016a)	0.020-0.167	9
47	C_9H_{12}	p-Ethyltoluene	0.060	(Li et al., 2016a)	0.039-0.122	6
48	C_9H_{12}	1,3,5-Trimethylbenzene	0.074	(Li et al., 2016a)	0.007-0.065	5
49	C_9H_{12}	o-Ethyltoluene	0.074	(Li et al., 2016a)	0.141-0.237	6
50	C_9H_{12}	1,2,4-Trimethylbenzene	0.074	(Li et al., 2016a)	0.028-0.065	9
51	C_9H_{12}	1,2,3-Trimethylbenzene	0.074	(Li et al., 2016a)	0.075-0.119	4
52	$C_{10}H_{14}$	m-Diethylbenzene	0.048	(Li et al., 2016a) (C10aromatics)	0.005-0.034	5
53	$C_{10}H_{14}$	p-Diethylbenzene	0.048		0.005-0.034	5
54	C_5H_8	Isoprene	0.440	(Kleindienst et al., 2006; Carlton et al., 2009)	0.003-0.017	11
55	$C_{10}H_{16}$	alpha-Pinene	0.346	(Ahlberg et al., 2017)	0.010-0.530	12
56	$C_{10}H_{16}$	beta-Pinene	0.346	Assumed as alpha-Pinene		
57	$C_{10}H_{16}$	Limonene	0.346	Assumed as alpha-Pinene		
58	C_4H_6O	Methacrolein	/			
59	C_4H_6O	Methyl vinyl ketone	/			
60	C_3H_4O	Acrolein	/			
61	C_3H_6O	Propanal	/			
62	C_3H_6O	Acetone	/			
63	C_4H_6O	Crotonaldehyde	/			
64	C_4H_8O	n-Butanal	/			
65	C_4H_8O	Methyl ethyl ketone	/			
66	$C_5H_{10}O$	2-Pentanone	/			
67	$C_5H_{10}O$	n-Pentanal	/			
68	$C_5H_{10}O$	3-Pentanone	/			
69	C_2H_4O	Acetaldehyde	/			
70	CH_2O	Formaldehyde	/			
71	$C_3H_4O_2$	Methylglyoxal	/			
72	C_5H_4O	Cyclopentadienone	/			

73	C_5H_8O	EVK, cyclopentanone, dihydromethylfuran	/			
74	$C_6H_{12}O$	C6 carbonyls	/			
75	C_7H_6O	Benzaldehyde	0.200	Assumed as toluene		
76	C_4H_4O	Furan*	0.050	(Gómez Alvarez et al., 2009)	0.019-0.072	2
77	C_5H_6O	Methyl furan	0.070	(Gómez Alvarez et al., 2009)	0.055-0.085	2
78	$C_4H_4O_2$	Furanone	0.050	Assumed as furan		
79	$C_5H_4O_2$	Furfural	0.050	Assumed as furan		
80	C_6H_8O	Dimethylfuran	0.070	Assumed as Methyl furan		
81	$C_5H_6O_2$	2-Methanol furanone	/			
82	$C_7H_{10}O$	TriMetfuran	0.070	Assumed as Methyl furan		
83	$C_6H_8O_2$	DiMetfuranone	0.070	Assumed as Methyl furan		
84	C_8H_6O	Benzofuran	0.156	Assumed as Styrene		
85	$C_8H_{12}O$	Butylfuran	0.070	Assumed as Methyl furan		
86	C_6H_6O	Phenol	0.440	(Yee et al., 2013)	0.240-0.540	5
87	C_7H_8O	Cresols	0.360	(Henry et al., 2008)	0.000-0.420	25
88	$C_6H_6O_2$	Benzenediols, methylfurfural	0.370	(Nakao et al., 2011)[b]	0.390	1
89	$C_8H_{10}O$	C2 phenols	0.440	(Nakao et al., 2011)[b]	0.130-0.730	7
90	$C_7H_8O_2$	Guaiacol, methyl benzenediols	0.500	(Yee et al., 2013)	0.340-0.530	11
91	$C_9H_{12}O$	Trimethylphenol	0.440	Assumed as C2 phenols		
92	$C_{10}H_8O$	Naphthalenol	0.440	Assumed as C2 phenols		
93	$C_{10}H_{12}O$	Methyl chavicol	0.440	Assumed as C2 phenols		
94	$C_8H_{10}O_3$	Syringol	0.370	(Yee et al., 2013)	0.110-0.370	7
95	$C_{10}H_8$	Naphthalene*	0.263	(Chan et al., 2009)	0.190-0.300	5
96	$C_{10}H_{10}$	Dihydronaphthalene	0.348	Assumed as MeNap		
97	$C_{11}H_{10}$	Methylnaphthalene (MetNap)	0.348	(Chan et al., 2009)	0.190-0.450	8
98	$C_{12}H_8$	Acenaphthalene	0.072	(Shakya et al., 2010)	0.030-0.110	10
99	$C_{12}H_{10}$	Acenaphthene	0.280	(Shakya et al., 2010)	0.040-0.130	8
100	$C_{12}H_{12}$	Dimethylnaphthalene (diMetNap)	0.372	(Chan et al., 2009)	0.300-0.310	3
101	$C_{13}H_{10}$	Fluorene	0.372	Assumed as diMetNap		
102	$C_{14}H_{10}$	Phenanthrene, Anthracene	0.372	Assumed as diMetNap		
103	$C_{16}H_{10}$	Pyrene, Fluoranthene	0.372	Assumed as diMetNap		
104	C_8H_{18}	C8 Alkanes	0.017		~0.40	1
105	C_9H_{20}	C9 Alkanes	0.021	(Lim and Ziemann, 2009; Presto et al., 2010)	0.070	1
106	$C_{10}H_{22}$	C10 Alkanes	0.033		0.010-0.150	3
107	$C_{11}H_{24}$	C11 Alkanes	0.050		0.270	1
108	$C_{12}H_{26}$	C12 Alkanes	0.090	(Presto et al., 2010)	~0.01-0.09	8
109	$C_{13}H_{28}$	C13 Alkanes	0.220	(Presto et al., 2010)[a]		
110	$C_{14}H_{30}$	C14 Alkanes	0.300	(Presto et al., 2010)[a]		
111	$C_{15}H_{32}$	C15 Alkanes	0.340	(Presto et al., 2010)	~0.10-0.60	10
112	$C_{16}H_{34}$	C16 Alkanes	0.390	(Presto et al., 2010)[a]		
113	$C_{17}H_{36}$	C17 Alkanes	0.430	(Presto et al., 2010)	0.090-0.510	10
114	$C_{18}H_{38}$	C18 Alkanes	0.430	Assumed as C17 Alkanes		
115	$C_{19}H_{40}$	C19 Alkanes	0.430	Assumed as C17 Alkanes		
116	$C_{20}H_{42}$	C20 Alkanes	0.430	Assumed as C17 Alkanes		
117	$C_{21}H_{44}$	C21 Alkanes	0.430	Assumed as C17 Alkanes		
118	C_2H_3N	Acetonitrile	/			
119	C_2H_5N	Ethenamine	/			
120	C_2H_7N	C2 amines	/			
121	C_3H_3N	Acrylonitrile	/			
122	C_3H_5N	Propanenitrile	/			
123	C_3H_9N	C3 amines	/			
124	C_4H_5N	Pyrrole	/			
125	C_4H_7N	Dihydropyrrole, butane	/			

[a], SOA yields was estimated using the reported two-product parameters (Presto et al., 2010) which derived from the experimental yields of C12 alkanes and C17 alkanes.

[b], Only SOA yields in the absence of NO_x were reviewed, which probably underestimate the SOA formation potential (Nakao et al., 2011; Yee et al., 2013).

[c], "/" in the column "Yield" denotes that these species are not the potential SOA precursors.

Q7: Section 3.3: The authors cited literature information to get the EFs of anthracite and straw and then applied these values to estimate the ROG emissions of residential coal and straw combustion in mainland China.

Are the quantification of EFs from limited sources representative?

R:

The EFs in this study were derived from the reported EF of benzene and the emission ratios (ER) of other species to benzene obtained in this study. Thus, to discuss the representative of EFs used for the estimation of emissions, two aspects should be considered as below.

(1) The representativeness of the cited EF of benzene from the literature

The major studies of the EF of benzene from residential combustion were reviewed and listed in Table R4. It can be seen the EF of benzene from each type of coal combustion generally reached a reasonable level of agreement and values of anthracite / briquette coal combustion ranged from 2 to 14 mg/kg (Cai et al., 2019; Tsai et al., 2003), which were 1-2 magnitude lower than those of bituminous coal combustion (Liu et al., 2017; Liu et al., 2015; Cai et al., 2019; Tsai et al., 2003; Wang et al., 2013). Considering the coal samples tested in this study were anthracite and briquette coal, the present study cited the latest results of anthracite coal combustion from Cai et al. (2019) study, in which the anthracite coal samples were from the two major coal production regions, i.e. Ningxia and Guizhou, and these coal types were widely used in China (Cai et al., 2019; Li et al., 2016b).

In terms of straw combustion, the EF of benzene in 12 samples from 6 literatures in total were summarized in Table R4 (Stockwell et al., 2015; Wu et al., 2022; Hatch et al., 2017; Inomata et al., 2015; Koss et al., 2018; Tsai et al., 2003) and ranged from 73 mg/kg to 800 mg/kg, which had large variations among different studies probably due to the various types of straws and combustion conditions. Among them, 7 out of 12 samples were from China straw, and their EF of benzene generally reached a reasonable level of agreement expect those of wet straw combustion. The present study used the median value of the reported EF of benzene from straw combustion in China, being of 284 mg/kg, which was derived from the simulated real-world combustion in the FLAM-4 laboratory campaign (Stockwell et al., 2015).

Table R4. The emission factors (EFs, mg/kg) of benzene for coals and straws reported by other studies.

Fuel	Combustion facility	Combustion Stage	N[a]	EFs	Reference
Coal					
Anthracite coal (Ningxia/Guizhou)	commercial stove widely used in northern China	a complete burn cycle	5	2-4.8	Cai et al. (2019)
Briquette coal (honeycomb)	metal coal stove with/without a flue	a complete burn cycle	3	~2.7-14	Tsai et al. (2003)
Briquette coal	metal coal stove without flue	a complete burn cycle	1	7.4	Tsai et al. (2003)
Anthracite and bituminous coal	commercial stove widely used in northern China	residential burning condition	5	21.5	Wang et al. (2013)

Fuel	Combustion facility	Combustion Stage	N[a]	EFs	Reference
Bituminous coal (Shenmu/ Neimeng/ Unknown)	commercial stove widely used in northern China	a complete burn cycle	8	94-156	Cai et al. (2019)
Washed coal	metal coal stove with a flue	a complete burn cycle	1	440	Tsai et al. (2003)
Pulverized coal	metal coal stove or brick stove with a flue	a complete burn cycle	2	25.8-1050	Tsai et al. (2003)
Bituminous coal	commercial stove widely used in northern China	flaming or smoldering stage	10	58.2-622.2	Liu et al. (2017)
Bituminous coal	domestic cooking stoves	flaming or smoldering stage	/	71-724	Liu et al. (2015)
Straw					
Rice Straw (China)	a large indoor combustion room	simulated real-world conditions	9	284±115	Stockwell et al. (2015)
Corncob (China)	combustion chamber	simulated real-world conditions	5	190	Wu et al. (2022)
Rice Straw (China)	combustion chamber	mix of flaming and smoldering	1	167	Hatch & al. (2017)
Rice Straw (China)	a heat-resistant combustion box	flaming	6	250±100	Inomata et al. (2015)
Rice Straw (China)	a heat-resistant combustion box	smoldering	8	400±100	Inomata et al. (2015)
Rice Straw (China)	a heat-resistant combustion box	smoldering (wet fuel)	4	800±500	Inomata et al. (2015)
Rape Plant (China)	a heat-resistant combustion box	flaming	2	220	Inomata et al. (2015)
Rape Plant (China)	a heat-resistant combustion box	smoldering	4	300±100	Inomata et al. (2015)
Wheat Straw	a large indoor combustion room	simulated real-world conditions	6	142±40	Stockwell et al. (2015)
wheat residue	brick stove with a flue	a complete burn cycle	1	512	Tsai et al. (2003)
maize residue	brick stove with a flue	a complete burn cycle	2	102-194	Tsai et al. (2003)
Rice Straw	Fire Sciences Laboratory facility	mix of flaming and smoldering	1	72.6	Koss et al. (2018)

[a], The number of samples.

(2) The reasonability of the ERs obtained in the present study

The ERs of ROG species to benzene obtained in this study were used to relate the ROG EFs especially previously unmeasured or rarely measured species emissions to benzene EF. The key point of the relating above was assuming the ERs obtained in this study were consistent with those of the previous studies. The consistence could be confirmed by the good correlation (R=0.73 for straw combustion, and R=0.82 for coal combustion) of the ERs of the overlapping species between our study and the previous studies, as shown in the Fig. S6 (a) and (e) in the Supplementary Information presented the correlation.

We have provided the discussions in the revised manuscript as following and in the Supplementary

Information:

Section 3.3, line 397-405:

"The major studies of the EF of benzene from residential combustion were further reviewed and listed in Table S4. Considering the coal samples tested in this study were anthracite and briquette coal, the present study cited the latest reported EF of benzene from anthracite coal combustion by Cai et al. (2019), which agreed with the other reported values of anthracite / briquette coal combustion (Tsai et al., 2003) and 1-2 magnitude lower than those of bituminous coal combustion (Liu et al., 2017; Liu et al., 2015; Cai et al., 2019; Tsai et al., 2003; Wang et al., 2013). In terms of straw combustion, the present study used the median value of the reported EF of benzene from straw combustion in China, being of 284 mg/kg, which was derived from the simulated real-world combustion in the FLAM-4 laboratory campaign (Stockwell et al., 2015). More particular consideration about selection of the reported EF of benzene was described in the Supplementing Information."

Section 2.3.4, line 408-414:

"To relate the ROG EFs especially previously unmeasured or rarely measured species emissions to benzene EF, the ER of ROG species to benzene was the ratio of their concentrations in the sample, and the average ER in different samples of each type of fuel was used in this study, as listed in Table S5. The key point of the relating above was assuming the ERs obtained in this study were consistent with those of the previous studies. The consistence could be confirmed by the good correlation (R=0.73 for straw combustion, and R=0.82 for coal combustion) of the ERs of the overlapping species between our study and the previous studies, as shown in the Fig. S6 (a) and (e) in the Supplementary Information presented the correlation."

Is anthracite representative of residential coal combustion in mainland China?

R:

Through an extensive literature search, little statistical data about the consumption of bituminous and anthracite coal in the residential sector of China was founded. From the rural energy survey in 2013-2014, the raw coal contributed 97% and 55% of the residential coal consumptions (raw coal and honeycomb briquette) in Baoding (Zhi et al., 2017; Zhi et al., 2015) and Beijing (Zhao et al., 2015), respectively. Assuming that the raw coal is equivalent to bituminous coal, the proportions of bituminous coal can be obtained roughly (Cai et al., 2019). China has been carrying out toughest-ever clean energy substitution and vigorously replacing bituminous coal with anthracite in response to the clean action plan in the residential sector since 2013, which were further strengthened from 2017 to 2020 during the three-year battle against air pollution. National Energy Administration strictly prohibit the sale of low rank coal in Action Plan for Clean and Efficient Utilization of Coal (2015-2020) (http://zfxxgk.nea.gov.cn/). The use and sale of bituminous coal were generally not allowed (Luo, 2019).

Thus, we could expect the large decrease of the use of bituminous coal in residential sector in China although there is no updated statistical data appliable. This study assumed that anthracite is the main residential coal type to roughly estimate ROG emissions in China. Even if the emission factors of

bituminous coal were applied, the ROG emissions from residential coal combustion in China would increase by approximately 1-2 orders of magnitude, which were still lower than the ROG emissions from biomass combustion. More refined energy consumption statistics are necessary to update as adjustment of Chinese energy structure, which is beyond the scope of our effort.

We have stressed the assumption in Section 3.3 and Fig. 5 in the revised manuscript as following:

"Notably, the appliable data about the contribution of bituminous and anthracite coal were from the rural energy survey conducted about ten years ago (2013-2014), which indicated the bituminous coal contributed 97% and 55% of the residential coal consumptions in Baoding (Zhi et al., 2017; Zhi et al., 2015) and Beijing (Zhao et al., 2015). China has been carrying out toughest-ever clean energy substitution and vigorously replacing bituminous coal with anthracite in response to the cleaning action plan in the residential sector since 2013, which were further strengthened from 2017 to 2020 during the three-year battle against air pollution (eg. Action Plan for Clean and Efficient Utilization of Coal (2015-2020), http://zfxxgk.nea.gov.cn/). The use and sale of bituminous coal were generally not allowed (Luo, 2019). Thus, we could expect the large decrease of the use of bituminous coal in residential sector in China although there is no updated statistical data appliable. This study assumed that anthracite is the main residential coal type to roughly estimate ROG emissions in China.

…Even if the emission factors of bituminous coal were applied, the ROG emissions from residential coal combustion in China would increase by approximately 1-2 orders of magnitude, which were still lower than the ROG emissions from biomass combustion. More refined energy consumption statistics are necessary to update as adjustment of Chinese energy structure."

Reference

Ahlberg, E., Falk, J., Eriksson, A., Holst, T., Brune, W. H., Kristensson, A., Roldin, P., and Svenningsson, B.: Secondary organic aerosol from VOC mixtures in an oxidation flow reactor, Atmospheric Environment, 161, 210-220, 10.1016/j.atmosenv.2017.05.005, 2017.

Akherati, A., He, Y., Coggon, M. M., Koss, A. R., Hodshire, A. L., Sekimoto, K., Warneke, C., de Gouw, J., Yee, L., Seinfeld, J. H., Onasch, T. B., Herndon, S. C., Knighton, W. B., Cappa, C. D., Kleeman, M. J., Lim, C. Y., Kroll, J. H., Pierce, J. R., and Jathar, S. H.: Oxygenated aromatic compounds are important precursors of secondary organic aerosol in biomass-burning emissions, Environ Sci Technol, doi.10.1021/acs.est.1020c01345, 10.1021/acs.est.0c01345, 2020.

Batterman, S. A., Zhang, G.-Z., and Baumann, M.: Analysis and stability of aldehydes and terpenes in electropolished canisters, Atmospheric Environment, 32, 1647-1655, https://doi.org/10.1016/S1352-2310(97)00417-2, 1998.

Bruns, E. A., El Haddad, I., Slowik, J. G., Kilic, D., Klein, F., Baltensperger, U., and Prevot, A. S. H.: Identification of significant precursor gases of secondary organic aerosols from residential wood combustion, Scientific Reports, 6, 10.1038/srep27881, 2016.

Bruns, E. A., Slowik, J. G., El Haddad, I., Kilic, D., Klein, F., Dommen, J., Temime-Roussel, B., Marchand, N., Baltensperger, U., and Prevot, A. S. H.: Characterization of gas-phase organics using proton transfer reaction time-of-flight mass spectrometry: fresh and aged residential wood combustion

emissions, Atmospheric Chemistry and Physics, 17, 705-720, 10.5194/acp-17-705-2017, 2017.

Cai, S., Zhu, L., Wang, S., Wisthaler, A., Li, Q., Jiang, J., and Hao, J.: Time-Resolved Intermediate-Volatility and Semivolatile Organic Compound Emissions from Household Coal Combustion in Northern China, Environmental Science & Technology, 53, 9269-9278, 10.1021/acs.est.9b00734, 2019.

Carlton, A. G., Wiedinmyer, C., and Kroll, J. H.: A review of Secondary Organic Aerosol (SOA) formation from isoprene, Atmospheric Chemistry and Physics, 9, 4987-5005, 2009.

Chan, A. W. H., Kautzman, K. E., Chhabra, P. S., Surratt, J. D., Chan, M. N., Crounse, J. D., Kuerten, A., Wennberg, P. O., Flagan, R. C., and Seinfeld, J. H.: Secondary organic aerosol formation from photooxidation of naphthalene and alkylnaphthalenes: implications for oxidation of intermediate volatility organic compounds (IVOCs), Atmospheric Chemistry and Physics, 9, 3049-3060, 10.5194/acp-9-3049-2009, 2009.

Cheng, P., Liu, Z., Feng, Y., Han, Y., Peng, Y., Cai, J., and Chen, Y.: Emission characteristics and formation pathways of carbonyl compounds from the combustion of biomass and their cellulose, hemicellulose, and lignin at different temperatures and oxygen concentrations, Atmospheric Environment, 291, 119387, https://doi.org/10.1016/j.atmosenv.2022.119387, 2022.

Gao, Y., Wang, H., Zhang, X., Jing, S., Peng, Y., Qiao, L., Zhou, M., Huang, D. D., Wang, Q., Li, X., Li, L., Feng, J., Ma, Y., and Li, Y.: Estimating Secondary Organic Aerosol Production from Toluene Photochemistry in a Megacity of China, Environ Sci Technol, 53, 8664-8671, 10.1021/acs.est.9b00651, 2019.

Gilman, J. B., Lerner, B. M., Kuster, W. C., Goldan, P. D., Warneke, C., Veres, P. R., Roberts, J. M., de Gouw, J. A., Burling, I. R., and Yokelson, R. J.: Biomass burning emissions and potential air quality impacts of volatile organic compounds and other trace gases from fuels common in the US, Atmospheric Chemistry and Physics, 15, 13915-13938, 10.5194/acp-15-13915-2015, 2015.

Gómez Alvarez, E., Borrás, E., Viidanoja, J., and Hjorth, J.: Unsaturated dicarbonyl products from the OH-initiated photo-oxidation of furan, 2-methylfuran and 3-methylfuran, Atmospheric Environment, 43, 1603-1612, https://doi.org/10.1016/j.atmosenv.2008.12.019, 2009.

Hatch, L. E., Yokelson, R. J., Stockwell, C. E., Veres, P. R., Simpson, I. J., Blake, D. R., Orlando, J. J., and Barsanti, K. C.: Multi-instrument comparison and compilation of non-methane organic gas emissions from biomass burning and implications for smoke-derived secondary organic aerosol precursors, Atmospheric Chemistry and Physics, 17, 1471-1489, 10.5194/acp-17-1471-2017, 2017.

Henry, F., Coeur-Tourneur, C., Ledoux, F., Tomas, A., and Menu, D.: Secondary organic aerosol formation from the gas phase reaction of hydroxyl radicals with m-, o- and p-cresol, Atmospheric Environment, 42, 3035-3045, https://doi.org/10.1016/j.atmosenv.2007.12.043, 2008.

Huo, Y., Guo, Z., Liu, Y., Wu, D., Ding, X., Zhao, Z., Wu, M., Wang, L., Feng, Y., Chen, Y., Wang, S., Li, Q., and Chen, J.: Addressing Unresolved Complex Mixture of I/SVOCs Emitted From Incomplete Combustion of Solid Fuels by Nontarget Analysis, Journal of Geophysical Research: Atmospheres, 126, 10.1029/2021jd035835, 2021.

Inomata, S., Tanimoto, H., Pan, X., Taketani, F., Komazaki, Y., Miyakawa, T., Kanaya, Y., and Wang, Z.: Laboratory measurements of emission factors of nonmethane volatile organic compounds from burning

of Chinese crop residues, Journal of Geophysical Research: Atmospheres, 120, 5237-5252, 10.1002/2014jd022761, 2015.

Jathar, S. H., Gordon, T. D., Hennigan, C. J., Pye, H. O. T., Pouliot, G., Adams, P. J., Donahue, N. M., and Robinson, A. L.: Unspeciated organic emissions from combustion sources and their influence on the secondary organic aerosol budget in the United States, Proceedings of the National Academy of Sciences, 111, 10473-10478, doi:10.1073/pnas.1323740111, 2014.

Jobson, B., Volkamer, R., Velasco, E., and Allwine, G.: Comparison of aromatic hydrocarbon measurements made by PTR-MS, DOAS and GC-FID during the MCMA 2003 Field Experiment, Atmospheric Chemistry and Physics, 10, 899-915, 2009.

Kleindienst, T. E., Edney, E. O., Lewandowski, M., Offenberg, J. H., and Jaoui, M.: Secondary organic carbon and aerosol yields from the irradiations of isoprene and alpha-pinene in the presence of NOx and SO2, Environmental Science & Technology, 40, 3807-3812, 10.1021/es052446r, 2006.

Koss, A. R., Warneke, C., Yuan, B., Coggon, M. M., Veres, P. R., and de Gouw, J. A.: Evaluation of NO+ reagent ion chemistry for online measurements of atmospheric volatile organic compounds, Atmospheric Measurement Techniques, 9, 2909-2925, 10.5194/amt-9-2909-2016, 2016.

Koss, A. R., Sekimoto, K., Gilman, J. B., Selimovic, V., Coggon, M. M., Zarzana, K. J., Yuan, B., Lerner, B. M., Brown, S. S., Jimenez, J. L., Krechmer, J., Roberts, J. M., Warneke, C., Yokelson, R. J., and de Gouw, J.: Non-methane organic gas emissions from biomass burning: identification, quantification, and emission factors from PTR-ToF during the FIREX 2016 laboratory experiment, Atmospheric Chemistry and Physics, 18, 3299-3319, 10.5194/acp-18-3299-2018, 2018.

Krechmer, J., Lopez-Hilfiker, F., Koss, A., Hutterli, M., Stoermer, C., Deming, B., Kimmel, J., Warneke, C., Holzinger, R., Jayne, J., Worsnop, D., Fuhrer, K., Gonin, M., and de Gouw, J.: Evaluation of a New Reagent-Ion Source and Focusing Ion-Molecule Reactor for Use in Proton-Transfer-Reaction Mass Spectrometry, Anal. Chem., 90, 12011-12018, 10.1021/acs.analchem.8b02641, 2018.

Li, H., Riva, M., Rantala, P., Heikkinen, L., Daellenbach, K., Krechmer, J. E., Flaud, P.-M., Worsnop, D., Kulmala, M., Villenave, E., Perraudin, E., Ehn, M., and Bianchi, F.: Terpenes and their oxidation products in the French Landes forest: insights from Vocus PTR-TOF measurements, Atmospheric Chemistry and Physics, 20, 1941-1959, 10.5194/acp-20-1941-2020, 2020.

Li, J., Zhang, H., Li, L., Ye, F., Wang, H., Guo, S., Zhang, N., Qin, M., and Hu, J.: Modeling Secondary Organic Aerosols in China: State of the Art and Perspectives, Current Pollution Reports, 10.1007/s40726-022-00246-3, 2023.

Li, L., Tang, P., Nakao, S., Kacarab, M., and Cocker, D. R., III: Novel Approach for Evaluating Secondary Organic Aerosol from Aromatic Hydrocarbons: Unified Method for Predicting Aerosol Composition and Formation, Environmental Science & Technology, 50, 6249-6256, 10.1021/acs.est.5b05778, 2016a.

Li, Q., Jiang, J., Zhang, Q., Zhou, W., Cai, S., Duan, L., Ge, S., and Hao, J.: Influences of coal size, volatile matter content, and additive on primary particulate matter emissions from household stove combustion, Fuel, 182, 780-787, https://doi.org/10.1016/j.fuel.2016.06.059, 2016b.

Lim, Y. B. and Ziemann, P. J.: Effects of Molecular Structure on Aerosol Yields from OH Radical-Initiated Reactions of Linear, Branched, and Cyclic Alkanes in the Presence of NOx, Environmental

Science & Technology, 43, 2328-2334, 10.1021/es803389s, 2009.

Liu, C., Zhang, C., Zhang, Y., and Mu, Y.: Preliminary study on volatile organic compounds emission from domestic cooking stoves under different coal combustion modes, The 16th Annual Academic Meeting of Chinese Society for Mineralogy Petrology and Geochemistry, Changchun, China, 2015.

Liu, C., Zhang, C., Mu, Y., Liu, J., and Zhang, Y.: Emission of volatile organic compounds from domestic coal stove with the actual alternation of flaming and smoldering combustion processes, Environmental pollution, 221, 385-391, 10.1016/j.envpol.2016.11.089, 2017.

Liu, Y., Shao, M., Fu, L., Lu, S., Zeng, L., and Tang, D.: Source profiles of volatile organic compounds (VOCs) measured in China: Part I, Atmospheric Environment, 42, 6247-6260, 10.1016/j.atmosenv.2008.01.070, 2008.

Luo, Y.: Research on the quality control of civil coal and interpretation of national standard, China Coal, 45, 14-18, 2019.

Mo, Z., Shao, M., and Lu, S.: Compilation of a source profile database for hydrocarbon and OVOC emissions in China, Atmospheric Environment, 143, 209-217, 10.1016/j.atmosenv.2016.08.025, 2016.

Nakao, S., Clark, C. H., Tang, P., Sato, K., and Cocker, D. R.: Secondary organic aerosol formation from phenolic compounds in the absence of NOx, Atmospheric Chemistry and Physics, 11, 10649-10660, 2011.

Ng, N. L., Kroll, J. H., Chan, A. W. H., Chhabra, P. S., Flagan, R. C., and Seinfeld, J. H.: Secondary organic aerosol formation from m-xylene, toluene, and benzene, Atmospheric Chemistry and Physics, 7, 3909-3922, 2007.

Presto, A. A., Miracolo, M. A., Donahue, N. M., and Robinson, A. L.: Secondary Organic Aerosol Formation from High-NOx Photo-Oxidation of Low Volatility Precursors: n-Alkanes, Environmental Science & Technology, 44, 2029-2034, 10.1021/es903712r, 2010.

Sekimoto, K., Li, S.-M., Yuan, B., Koss, A., Coggon, M., Warneke, C., and de Gouw, J.: Calculation of the sensitivity of proton-transfer-reaction mass spectrometry (PTR-MS) for organic trace gases using molecular properties, International Journal of Mass Spectrometry, 421, 71-94, 10.1016/j.ijms.2017.04.006, 2017.

Stockwell, C. E., Veres, P. R., Williams, J., and Yokelson, R. J.: Characterization of biomass burning emissions from cooking fires, peat, crop residue, and other fuels with high-resolution proton-transfer-reaction time-of-flight mass spectrometry, Atmospheric Chemistry and Physics, 15, 845-865, 10.5194/acp-15-845-2015, 2015.

Tajuelo, M., Rodriguez, D., Teresa Baeza-Romero, M., Diaz-de-Mera, Y., Aranda, A., and Rodriguez, A.: Secondary organic aerosol formation from styrene photolysis and photooxidation with hydroxyl radicals, Chemosphere, 231, 276-286, 10.1016/j.chemosphere.2019.05.136, 2019.

Tsai, S. M., Zhang, J. J., Smith, K. R., Ma, Y., Rasmussen, R. A., and Khalil, M. A.: Characterization of non-methane hydrocarbons emitted from various cookstoves used in China, Environ Sci Technol, 37, 2869-2877, 10.1021/es026232a, 2003.

Wang, C., Yuan, B., Wu, C., Wang, S., Qi, J., Wang, B., Wang, Z., Hu, W., Chen, W., Ye, C., Wang, W., Sun, Y., Wang, C., Huang, S., Song, W., Wang, X., Yang, S., Zhang, S., Xu, W., Ma, N., Zhang, Z., Jiang,

B., Su, H., Cheng, Y., Wang, X., and Shao, M.: Measurements of higher alkanes using NO+ chemical ionization in PTR-ToF-MS: important contributions of higher alkanes to secondary organic aerosols in China, Atmos. Chem. Phys., 20, 14123-14138, 10.5194/acp-20-14123-2020, 2020.

Wang, Q., Geng, C., Lu, S., Chen, W., and Shao, M.: Emission factors of gaseous carbonaceous species from residential combustion of coal and crop residue briquettes, Frontiers of Environmental Science & Engineering, 7, 66-76, 10.1007/s11783-012-0428-5, 2013.

Wu, J., Kong, S., Yan, Y., Yao, L., Yan, Q., Liu, D., Shen, G., Zhang, X., and Qi, S.: Neglected biomass burning emissions of air pollutants in China-views from the corncob burning test, emission estimation, and simulations, Atmospheric Environment, 10.1016/j.atmosenv.2022.119082, 2022.

Yee, L. D., Kautzman, K. E., Loza, C. L., Schilling, K. A., Coggon, M. M., Chhabra, P. S., Chan, M. N., Chan, A. W. H., Hersey, S. P., Crounse, J. D., Wennberg, P. O., Flagan, R. C., and Seinfeld, J. H.: Secondary organic aerosol formation from biomass burning intermediates: phenol and methoxyphenols, Atmospheric Chemistry and Physics, 13, 8019-8043, 10.5194/acp-13-8019-2013, 2013.

Yuan, B., Koss, A. R., Warneke, C., Coggon, M., Sekimoto, K., and de Gouw, J. A.: Proton-Transfer-Reaction Mass Spectrometry: Applications in Atmospheric Sciences, Chemical Reviews, 117, 13187-13229, 10.1021/acs.chemrev.7b00325, 2017.

Zhang, X., Cappa, C. D., Jathar, S. H., McVay, R. C., Ensberg, J. J., Kleeman, M. J., and Seinfeld, J. H.: Influence of vapor wall loss in laboratory chambers on yields of secondary organic aerosol, Proceedings of the National Academy of Sciences of the United States of America, 111, 5802-5807, 10.1073/pnas.1404727111, 2014.

Zhao, W., Xu, Q., Li, L., Jiang, L., Zhang, D., and Chen, T.: Estimation of Air Pollutant Emissions from Coal Burning in the Semi-Rural Areas of Beijing Plain, Research of Environmental Sciences, 28, 869, 2015.

Zhi, G., Yang, J., Zhang, T., Guan, J., Du, J., Xue, Z., and Meng, F.: Rural Household Coal Use Survey, Emission Estimation and Policy Implications, Research of Environmental Sciences, 28, 1179, 2015.

Zhi, G., Zhang, Y., Sun, J., Cheng, M., Dang, H., Liu, S., Yang, J., Zhang, Y., Xue, Z., Li, S., and Meng, F.: Village energy survey reveals missing rural raw coal in northern China: Significance in science and policy, Environmental pollution, 223, 705-712, 10.1016/j.envpol.2017.02.009, 2017.